DHT-BASED FREQUENCY-DOMAIN EQUALIZER FOR DMT SYSTEMS

Chih-Feng Wu, †Muh-Tian Shiue and Chrong-Kuang Wang

Graduate Institute of Electronics Engineering and Department of Electrical Engineering,
National Taiwan University, Taipei, Taiwan
†Department of Electrical Engineering, National Central University, Chung-Li, Taiwan
email: cfwu@aic.ee.ntu.edu.tw, †mtshiue@ee.ncu.edu.tw and ckwang@cc.ee.ntu.edu.tw

ABSTRACT

A DHT-based frequency-domain equalizer (FEQ) is presented to eliminate the real-to-complex transformation (R2CT) for the discrete Hartley transform (DHT) based discrete multi-tone (DMT) systems. The DHT-based FEQ can be further used to develop the DHT-based per-tone equalization for DMT systems. In this paper, the DHT-based DMT ADSL system is adopted as a vehicle to demonstrate the DHT-based FEQ performance. Based on the steepest descent (SD) algorithm, the DHT-based FEQ is derived without employing R2CT, which costs $2N$-addition. N is the number of DHT points. The performance analysis of the DHT-based FEQ proves no signal-to-noise ratio (SNR) loss compared with the DFT-based FEQ, and the bit allocation and data rate are identical with the performance analysis.

1. INTRODUCTION

DMT, which is one of the multi-carrier modulation (MCM) techniques [2], has been applied to broadband wireline transmission over the twisted-pair telephone line such as ADSL, ADSL2, ADSL2+ and VDSL. Referring to [3], a typical DMT-based ADSL system model is shown in Fig. 1. The time-domain equalizer (TEQ) is used to shorten the channel dispersion. It minimizes the intersymbol interference (ISI) caused by the channel distortions such as loop length, gauge-change and bridge-tap. Although the TEQ can minimize the ISI in time domain, the phase rotation and amplitude attenuation in frequency domain still exist on each subchannel. In order to overcome these distortions, an FEQ is employed to compensate for the channel distortions on each subchannel.

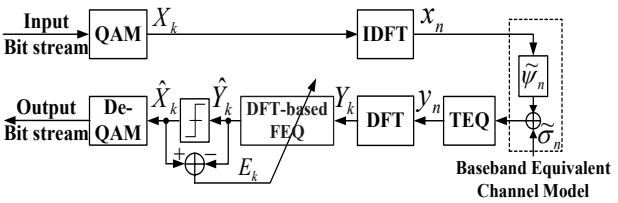

Figure 1: Typical DFT-based DMT ADSL system model.

The IDFT/DFT [1] can be adopted to perform the baseband modulation/demodulation for the MCM systems. In addition, an equalization that is based on the SD algorithm is also presented to combat the channel distortions on each subchannel. Such an equalizer can be called the DFT-based FEQ as shown in Fig. 1. In practice, the fast fourier transform (FFT)/inverse FFT (IFFT) can substitute for the DFT/IDFT to reduce the complex multiplication from N^2 to $\frac{N}{2}log_2N$ (radix-2).

This work was supported by NSC, Taiwan, under grant NSC 93-2213-E-002-001 and NSC92-2218-E-008-010.

Considering the prior arts [4]-[7], the baseband modulation/demodulation is performed by IDHT/DHT and C2RT/R2CT [8] to decrease the computing complexity from complex multiplication to real multiplication since the IDHT/DHT is real-valued operation. The C2RT is required to transform a complex symbol into a real symbol since the subchannel transmission symbol is QAM symbol. Inversely, the R2CT transforms a real symbol to a complex symbol. Although the DFT/FFT is replaced by the DHT, the FEQ architecture is still the conventional DFT-based FEQ as shown in Fig. 2.

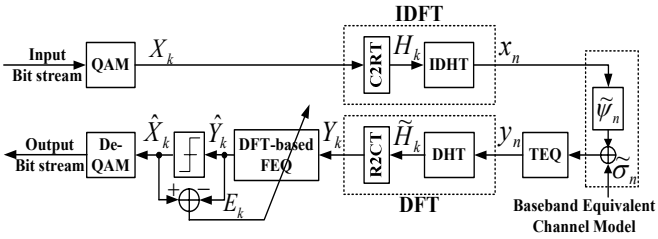

Figure 2: DHT-based DMT ADSL system model.

In this paper, based on the DHT-based DMT systems, an alternative FEQ is proposed since the DFT/FFT is replaced by DHT without employing R2CT. The DHT-based FEQ can be extended straightforward to design the DHT-based per-tone equalization.In practice, the DHT-based FEQ equalizes the DHT tone from 0th to $(N-1)$th. The DFT-based FEQ, on the other hand, equalizes the DFT tone from 0th to $(\frac{N}{2}-1)$th. Consequently, the computing complexity and subchannel SNR of the DHT-based FEQ are consistent with the DFT-based FEQ. This paper is organized as follows: the analytical models of DFT and DHT are introduced in seciton 2. The DHT-based FEQ are derived in section 3. The simulation results are shown in section 4. Finally, conclusions are given in section 5.

2. ANALYTICAL MODELS

2.1 DFT

Considering the DFT-based DMT systems, the N-point IDFT and DFT are given by

$$x_n = \frac{1}{N}\sum_{k=0}^{N-1} X_k W_N^{-kn}, n = 0, 1, ..., N-1 \quad (1)$$

$$X_k = \sum_{n=0}^{N-1} x_n W_N^{nk}, k = 0, 1, ..., N-1 \quad (2)$$

where $W_N = e^{-j\frac{2\pi}{N}}$, X_k is a complex transmission symbol on the kth subchannel in frequency-domain and x_n is the nth transmission sample in time-domain. Theoretically, if

x_n is a real-valued sequence, X_k has a property of conjugate symmetry, namely, $X_{N-k} = X_k^*$ for $0 \leq k \leq (\frac{N}{2} - 1)$, where asterisk denotes the complex conjugate. Besides, the shift property is given by

$$x_{n-m} \overset{DFT}{\longleftrightarrow} e^{-j\theta_{mk}} X_k \tag{3}$$

where $\theta_{mk} = (2\pi mk/N)$ and m is a delay index. Obviously, the shift property describes a shift sequence, x_{n-m}, in time-domain leads to a phase rotation in frequency-domain.

2.2 DHT

Similarly, considering the DHT-based DMT systems, the N-point IDHT and DHT are defined by

$$x_n = \frac{1}{N} \sum_{k=0}^{N-1} H_k cas(2\pi kn/N), n = 0, 1, ..., N-1 \tag{4}$$

$$H_k = \sum_{n=0}^{N-1} x_n cas(2\pi nk/N), k = 0, 1, ..., N-1 \tag{5}$$

where $cas(\cdot) = cos(\cdot) + sin(\cdot)$ and H_k is the real transmission symbol of the kth subchannel in frequency domain. In addition, the shift property [8] of DHT is given by

$$x_{n-m} \overset{DHT}{\longleftrightarrow} cos(\theta_{mk}) H_k - sin(\theta_{mk}) H_{N-k} \tag{6}$$

Eq. (6) shows that a shift sequence in time-domain gives rise to a phase rotation in frequency-domain. The phase rotation is composed of cosine and sine coefficient. Particularly, the sine coefficient has a backward feature.

2.3 Relationship of DFT and DHT

In fact, the conversion between DFT and DHT can be achieved by a transformation matrix, T, which is given by

$$T = \begin{bmatrix} 1/2 & 1/2 \\ -1/2 & 1/2 \end{bmatrix} \tag{7}$$

In addition, T has an identical inverse, $\overline{T}$, which is given by

$$\overline{T} = \begin{bmatrix} 1 & -1 \\ 1 & 1 \end{bmatrix} \tag{8}$$

Consequently, the H_k and H_{N-k} are derived by

$$\begin{bmatrix} H_k \\ H_{N-k} \end{bmatrix} = \begin{bmatrix} 1 & -1 \\ 1 & 1 \end{bmatrix} \begin{bmatrix} X_{k,R} \\ X_{k,I} \end{bmatrix} \tag{9}$$

where $X_k = X_{k,R} + jX_{k,I}$. Eq. (9) is true if and only if the conjugate symmetry property is existence. Therefore, $\overline{T}$ can be called the C2RT, which describes a symbol transformation from complex to real on the kth subchannel. Conversely, the $X_{k,R}$ and $X_{k,I}$ can be derived by

$$\begin{bmatrix} X_{k,R} \\ X_{k,I} \end{bmatrix} = \begin{bmatrix} 1/2 & 1/2 \\ -1/2 & 1/2 \end{bmatrix} \begin{bmatrix} H_k \\ H_{N-k} \end{bmatrix} \tag{10}$$

Therefore, Eq. (10) can be called R2CT, which expresses the symbol transformation from a real symbol to a complex symbol.

From Eq. (9) and (10), it is clear that the $X_{k,R}$ and $X_{k,I}$ can be viewed as a basis of the symbol transformation and the H_k and H_{N-k} are obtained by the linear combination of the $X_{k,R}$ and $X_{k,I}$, and vice versa.

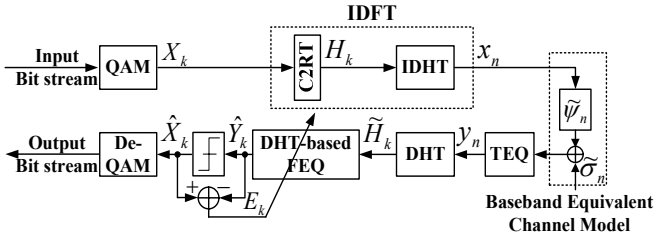

Figure 3: Proposed DHT-based FEQ for DMT ADSL system model.

3. DHT-BASED FEQ

[6] and [7] proposed the DHT-based FFT/IFFT processor to reduce the FFT/IFFT complexity for the DMT-based xDSL systems as shown in Fig. 2. However, from the system point of view, the FEQ architecture is still the conventional DFT-based FEQ. Therefore, a DHT-based FEQ is proposed to remove the R2CT for DMT systems as shown in Fig. 3.

Based on the discussion in section 2, in addition to that a shift of transmitted signal in time-domain is induced by the transmission channel, the channel in general results in dispersion of the transmission signals in time-domain. Consequently, the dispersion channel gives rise to impairments that include phase rotation and amplitude attenuation of the signals in frequency-domain. Both Eq. (3) and (6), therefore, have to be modified with amplitude attenuation as described in the following subsections.

3.1 DFT-based

Considering the dispersion channel, which is composed of baseband equivalent channel model and TEQ, the input of FEQ can be described as follows:

$$Y_k = A_{mk} e^{-j\theta_{mk}} X_k \tag{11}$$

where A_{mk} and θ_{mk} describe the amplitude and phase distortions respectively due to dispersion channel. Without losing the generality, the baseband equivalent noise ($\tilde{\sigma}_n$) is not considered in Eq. (11).

The FEQ minimizes the minimum mean-square distortions such as phase rotation and amplitude attenuation on each subchannel. The $W_k^{\mathcal{F}}$ coefficient of DFT-based FEQ is chosen to minimize the minimum mean-square error and given by

$$W_k^{\mathcal{F}} = \hat{A}_{mk} e^{j\hat{\theta}_{mk}} \tag{12}$$

where $\hat{A}_{mk}$ and $\hat{\theta}_{mk}$ express the compensations of amplitude and phase distortions respectively. The notation, $\mathcal{F}$, denotes the DFT-based. The cost function of minimum mean-square estimation (MMSE), $\varepsilon_{k,\mathcal{F}}$, on each subchannel is given by

$$\varepsilon_{k,\mathcal{F}} = E[e_{k,\mathcal{F}} e_{k,\mathcal{F}}^*] \tag{13}$$

where $e_{k,\mathcal{F}} = X_k - \hat{Y}_k^{\mathcal{F}}$ and $E[\cdot]$ is an expectation operator. In practice, the DFT-based FEQ coefficient, $W_k^{\mathcal{F}} = W_{k,R} + jW_{k,I}$, is used and the matrix form of the DFT-based FEQ output is defined by

$$\begin{bmatrix} \hat{Y}_{k,R}^{\mathcal{F}} \\ \hat{Y}_{k,I}^{\mathcal{F}} \end{bmatrix} = \begin{bmatrix} W_{k,R} & W_{k,I} \\ -W_{k,I} & W_{k,R} \end{bmatrix} \begin{bmatrix} Y_{k,R} \\ Y_{k,I} \end{bmatrix} \tag{14}$$

where $\hat{Y}_k^{\mathcal{F}} = \hat{Y}_{k,R}^{\mathcal{F}} + j\hat{Y}_{k,I}^{\mathcal{F}}$ and $Y_k = Y_{k,R} + jY_{k,I}$. The coefficients updating can be obtained by

$$\begin{bmatrix} W_{k,R}(n+1) \\ W_{k,I}(n+1) \end{bmatrix} = \begin{bmatrix} W_{k,R}(n) \\ W_{k,I}(n) \end{bmatrix} + \mu_{k,\mathcal{F}} \begin{bmatrix} e_{k,R} Y_{k,R} + e_{k,I} Y_{k,I} \\ e_{k,R} Y_{k,I} - e_{k,I} Y_{k,R} \end{bmatrix} \tag{15}$$

where $\mu_{k,\mathcal{F}}$ is the step-size of the DFT-based FEQ.

3.2 DHT-based

Considering the DHT-based DMT systems as shown in Fig. 3, the dispersion channel is assumed the same as that used in subsection 3.1. The DHT output can be derived and expressed in matrix form as follows:

$$\begin{bmatrix} \tilde{H}_k \\ \tilde{H}_{N-k} \end{bmatrix} = B_{mk} \begin{bmatrix} cos(\theta_{mk}) & -sin(\theta_{mk}) \\ sin(\theta_{mk}) & cos(\theta_{mk}) \end{bmatrix} \begin{bmatrix} H_k \\ H_{N-k} \end{bmatrix} \quad (16)$$

where B_{mk} and θ_{mk} denote the amplitude and phase distortions on each tone of DHT output. Hence, the DHT-based FEQ is required to compensate for the distortions on each tone for $0 \leq k \leq (N-1)$.

Similarly, the coefficients of DHT-based FEQ, S_k and C_k, are given by

$$S_k = \hat{B}_{mk} cas(\hat{\theta}_{mk}) \quad (17)$$

$$C_k = \hat{B}_{mk} cas'(\hat{\theta}_{mk}) \quad (18)$$

where $cas'(\cdot) = cos(\cdot) - sin(\cdot)$. $\hat{B}_{mk}$ and $\hat{\theta}_{mk}$ express the compensations of amplitude and phase distortions respectively. In order to obtain the optimal solution of S_k and C_k, the cost function of MMSE, $\varepsilon_{k,\mathcal{H}}$, on each subchannel is defined as follows:

$$\varepsilon_{k,\mathcal{H}} = E[e_{k,\mathcal{H}} e^*_{k,\mathcal{H}}] \quad (19)$$

where $e_{k,\mathcal{H}} = X_k - \hat{Y}_k^{\mathcal{H}}$. The notation, $\mathcal{H}$, denotes the DHT-based. Therefore, the matrix form of the output for DHT-based FEQ is described by

$$\begin{bmatrix} \hat{Y}_{k,R}^{\mathcal{H}} \\ \hat{Y}_{k,I}^{\mathcal{H}} \end{bmatrix} = \begin{bmatrix} S_k & C_k \\ -C_k & S_k \end{bmatrix} \begin{bmatrix} \tilde{H}_k \\ \tilde{H}_{N-k} \end{bmatrix} \quad (20)$$

where $\hat{Y}_k^{\mathcal{H}} = \hat{Y}_{k,R}^{\mathcal{H}} + j\hat{Y}_{k,I}^{\mathcal{H}}$. Using the SD algorithm to obtain the optimal solution of S_k and C_k to minimize the MMSE, the gradient of $\varepsilon_{k,\mathcal{H}}$ with respect to S_k and C_k can be shown as

$$(\nabla \varepsilon_{k,\mathcal{H}})_{S_k} = \frac{\partial}{\partial S_k} \varepsilon_{k,\mathcal{H}} = -2E[e_{k,R}\tilde{H}_k + e_{k,I}\tilde{H}_{N-k}] \quad (21)$$

$$(\nabla \varepsilon_{k,\mathcal{H}})_{C_k} = \frac{\partial}{\partial C_k} \varepsilon_{k,\mathcal{H}} = -2E[e_{k,R}\tilde{H}_{N-k} + e_{k,I}\tilde{H}_k] \quad (22)$$

The SD algorithm makes changes in an opposite direction of the gradient

$$S_k(n+1) = S_k(n) + \mu_{k,\mathcal{H}}[\frac{1}{2}(-\nabla \varepsilon_{k,\mathcal{H}})_{S_k}] \quad (23)$$

$$C_k(n+1) = C_k(n) + \mu_{k,\mathcal{H}}[\frac{1}{2}(-\nabla \varepsilon_{k,\mathcal{H}})_{C_k}] \quad (24)$$

where $\mu_{k,\mathcal{H}}$ is the step-size of the DHT-based FEQ. The block diagram is shown in Fig. 4.

3.3 Subchannel SNR Consideration

The subchannel performance is defined by the geometric SNR [2] and given by

$$SNR_k = \frac{\epsilon_k |\Psi_k|^2}{\sigma_k^2} \quad (25)$$

where ϵ_k, Ψ_k and σ_k denote the transmitted symbol energy, target channel response and standard deviation of target channel noise on the kth subchannel respectively. Since Eq. (25) can not be obtained directly, the SNR_k can be measured by

$$SNR_k = \frac{P_k}{N_k} = \frac{|X_k|^2}{|e_k|^2} \quad (26)$$

where P_k and N_k are the signal and noise power of the kth subchannel respectively. Furthermore, the SNR_k is evaluated at the end of the transceiver training and channel analysis phase of initialization. Therefore, the P_k is a fixed value, which is the power of the training symbol, and N_k is the power of $e_{k,\mathcal{F}}$ or $e_{k,\mathcal{H}}$.

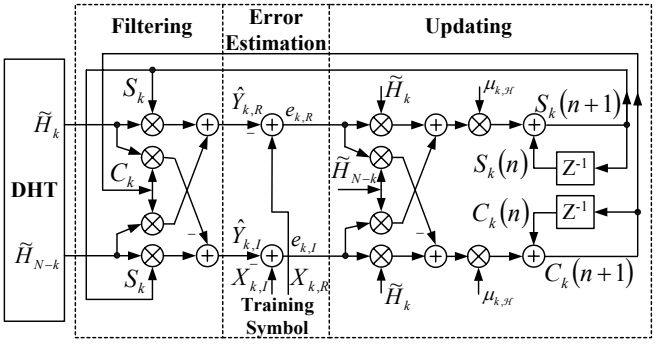

Figure 4: Block diagram of the DHT-based FEQ.

Essentially, both DFT-based FEQ and DHT-based FEQ are a single-tap Wiener filter. If the updating step-sizes are carefully evaluated, both will converge to retrieve the transmitted data $X_{k,R}$ and $X_{k,I}$, that is, $Q\{\hat{Y}_{k,\mathcal{F}}\} = Q\{\hat{Y}_{k,\mathcal{H}}\} = X_k$, where $Q\{\cdot\}$ denotes the decision operator. Combining Eq. (14), (20) and (10), the following relationships can be shown:

$$S_k = (W_{k,R} - W_{k,I})/2 \quad (27)$$

$$C_k = (W_{k,R} + W_{k,I})/2 \quad (28)$$

$$\hat{B}_{mk} = \frac{\hat{A}_{mk}}{2} \quad (29)$$

According to Eq. (27), (28) and (29), $e_{k,\mathcal{F}}$ and $e_{k,\mathcal{H}}$ will be identical. Therefore, $N_{k,\mathcal{H}}$ is also equivalent to $N_{k,\mathcal{F}}$, namely, the DHT-based FEQ can achieve the same subchannel SNR with the DFT-based FEQ under the identical target channel response. From the system point of view, it can be concluded that the DHT-based FEQ can compensate for the phase and amplitude distortions with DFT-based FEQ, while the DFT is replaced by the DHT without employing R2CT.

4. SIMULATION RESULTS

4.1 Simulation Model

The DHT-based DMT ADSL system is adopted as a vehicle to demonstrate the DHT-based FEQ performance. A MATLAB program is developed for the DHT-based DMT ADSL system as shown in Fig. 2 and 3 to evaluate the performance between DFT-based FEQ and DHT-based FEQ. The standard LMS algorithm with the unit energy constraint of the target channel response is used to train TEQ coefficients. Besides, the back-ground noise power density is equivalent to -140-dBm/Hz over the receiver input impedance 100-Ω, which is defined in G.992.1 (ADSL standard). The channel impulse and frequency response of some test loops are shown in Fig. 5 (a) and (b).

In order to demonstrate the proposed architecture, there are 2 cases in simulation model. Both of the cases in transmit path consist of QAM, C2RT and IDHT as shown in Fig. 2. However, the receive path has a different architecture. In case I, the receive path is composed of TEQ, DHT, R2CT,

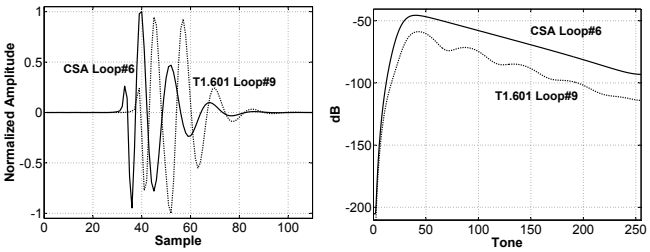

(a) (b)

Figure 5: (a). Channel impulse response and (b). frequency response of the T1.601 Loop#9 and CSA Loop#6.

DFT-based FEQ and de-QAM. In case II, the receive path includes TEQ, DHT, DHT-based FEQ and de-QAM. In each simulation, the FEQ training is designed to use 500-symbol in C-REVERB3. The bit allocations are obtained by the subchannel SNR measurement, which is calculated by integrate-and-dump using the last 100-symbol in C-REVER3.

4.2 Step-Size Selection and Comparisons

The subchannel step-size is determined by the results [9] for DFT/DHT-based FEQ and given by

$$\mu_{k,\mathcal{F}} = \frac{0.118}{Y_{k,R}^2 + Y_{k,I}^2} \tag{30}$$

$$\mu_{k,\mathcal{H}} = \frac{0.118}{\tilde{H}_k^2 + \tilde{H}_{N-k}^2} \tag{31}$$

It is clear that $\mu_{k,\mathcal{H}}$ is half of $\mu_{k,\mathcal{F}}$.

A comparison of the computing complexity in the receive path are listed in Table. 1, where just describes single tone operation requirement. The R2CT requires 2-addition for each tone since the $\frac{1}{2}$-term in Eq. (10) can be ignored easily for VLSI realization. From what has been derived above, it could be concluded that the computing complexity of DHT-based FEQ is the same as DFT-based FEQ.

Table 1: Comparisons in computing complexity.

Receive path computing complexity			DHT+R2CT DFT-based FEQ	DHT DHT-based FEQ
R2CT		+	2	–
SD algorithm	filtering	×	4	4
		+	2	2
	error estimation	+	2	2
	updating	×	4	4
		+	4	4

4.3 Simulation Results

Finally, the simulation results of the data rate for all test loops are listed in Table. 2. From the simulation results, it can be concluded that the performance analysis in section 3.3 is consistent with the simulation results. In addition, the bit allocation of the T1.601 Loop#9 and CSA Loop#6 is illustrated in Fig. 6 (a) and (b), which demonstrates the subchannel SNR is identical between DFT and DHT-based FEQ.

5. CONCLUSIONS

In this paper, an alternative DHT-based FEQ is proposed for DHT-based DMT systems since R2CT is excluded. Based on the SD algorithm, the architecture and performance of DHT-based FEQ are derived. Furthermore, the DHT-based DMT ADSL system is adopted as a vehicle to demonstrate the DHT-based FEQ architecture without SNR loss compared with DFT-based FEQ. The computing complexity of DHT-based FEQ is also the same as the DFT-based FEQ. Finally, the simulation results of both bit allocation and data rate

Table 2: Simulation results.

Test Loop	Case I REVERB (Kbps)	Case II REVERB (Kbps)
T1.601 Loop#7	3556	3556
T1.601 Loop#9	4560	4560
T1.601 Loop#13	4408	4408
CSA Loop#4	9864	9864
CSA Loop#6	9272	9272
CSA Loop#7	9176	9176
CSA Loop#8	8496	8496
mid-CSA Loop	12664	12664

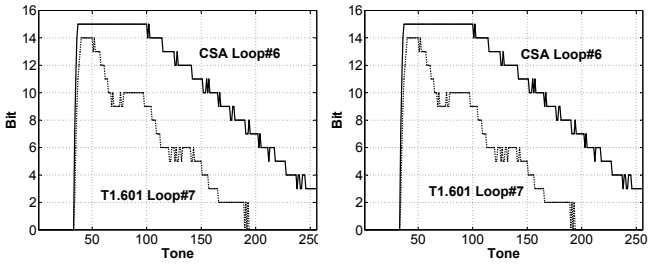

(a) (b)

Figure 6: Bit allocation of T1.601 Loop#9 and CSA Loop#6 for (a) DFT-bsed FEQ and (b) DHT-based FEQ

are consistent with the performance analysis. According to the DHT-based FEQ, the DHT-based per-tone equalization can be developed straightforward for DMT systems.

REFERENCES

[1] S. B. Weinstein and Paul M. Ebert, "Data Transmission by Frequency-Division Multiplexing Using the Discrete Fourier Transform," *IEEE Trans. on Commun. Tech.*, vol. COM-19, no. 5, Oct. 1971.

[2] John M. Cioffi, "A multicarrier primer," *ANSI T1E1.4 committee contribution*, pp. 19–37, Nov. 1991.

[3] John A. C. Bingham John M. Cioffi, "DMT specification overview for ADSL," *T1E1.4/93-083R2*, Aug. 23, 1993.

[4] Thomas Starr, John M. Cioffi and Peter Silverman, "Understanding Digital Subscriber Line Technology," Prentice Hall, pp. 224, 1999.

[5] C. L. Wang, C. H. Chang, J. L. Fan and J. M. Cioffi, "Discrete Hartley Transform Based Multicarrier Modulation," *IEEE ICASSP*, pp. 2513–2516, Jun. 2000.

[6] C. L. Wang and C. H. Chang, "A novel DHT-based FFT/IFFT processor for ADSL transceivers," *IEEE ISCAS*, pp. 51–54, May 1999.

[7] C. L. Wang and C. H. Chang, "A DHT-Based FFT/IFFT Processor for VDSL Transceivers," *IEEE ICASSP*, pp. 1213–1216, May 2001.

[8] R. N. Bracewell, "Discrete Hartley Transform," *J. Opt. Soc. Am.*, vol. 73, no. 12, pp. 1832–1835, Dec. 1983.

[9] C. F. Wu, M. T. Shiue and C. K. Wang, "On-Line Frequency-domain Equalizer Step-Size Calculation Using Signal Power Estimation-Tone Grouping for DMT-Based Systems," in *IEEE APCCAS 2004*, pp. 685-688, Dec. 2004